CRYSTAL DEVELOPMENT IN DISCOASTERACEAE AND BRAARUDOSPHAERACEAE (PLANKTONIC ALGAE)

by MAURICE BLACK

ABSTRACT. In both families the skeleton consists of little rosettes of calcite crystals grouped round a central axis. In the Discoasteraceae the crystals are arranged each with its optic axis parallel with the principal (= central) axis; the individual crystals have a bilateral symmetry with virtual suppression of the trigonal symmetry characteristic of inorganically grown crystals. The Braarudosphaeraceae differ in having their crystals arranged with a cleavage plane at right angles to the principal axis, to which the optic axes are oblique; the calcite is internally laminated parallel to this cleavage, and all three cleavages respond differently to etching. It is suggested that these peculiarities in morphology and chemical behaviour result from biochemical controls exerted by the organism during crystal growth, producing complex internal structures on a very fine scale, yet not fine enough to interfere with the crystal-lattice.

I HAVE commented elsewhere upon the remarkable control which coccolithophorid cells are able to exert over the crystallization of calcite, enabling them to shape the crystals that they secrete with great precision (Black 1963). Two other families of planktonic algae, the Discoasteraceae and Braarudosphaeraceae, share this ability to regulate the growth of crystal faces, and although the resulting patterns are different, the crystallographic control is equally striking.

At present we do not know how this is achieved. The physiological processes leading up to the precipitation of calcium carbonate in the coccolithophorid cell have been investigated in some detail (Paasche 1968, Watabe and Wilbur 1966), and the same general principles are presumably applicable to the discoasters and braarudosphaerids. The morphology of the resulting crystals, on the other hand, is clearly dependent upon controls of a much more specific kind; it is perhaps connected with biochemical peculiarities which are constant in any given species, but vary from one species to another and from one family to another. Looked at in this way, structural details of the crystalline skeleton may be expected to reflect biochemical characters, at present unknown, but likely to have an important bearing upon the taxonomy of these organisms.

TERMINOLOGY AND CHOICE OF INDICES

Miller's three-index notation for the trigonal system has considerable advantages over a four-index method for representing the crystal faces in the arms of a discoaster, and for this reason has been adopted here. When the rhombohedron face inclined towards the principal axis is taken as (010), the indices display the bilateral symmetry of a discoaster arm with a clarity that would be impossible if a four-index notation were used.

The word *face* is used in its crystallographical sense, and the obverse and reverse sides of the asterolith are referred to as *surfaces*. Since we do not know which of the two surfaces was external in relation to the cell, we cannot logically speak of them as upper and lower, or distal and proximal. The two surfaces are nevertheless morphologically

[Palaeontology, Vol. 15, Part 3, 1972, pp. 476–489, pls. 87–96.]

unlike, and we can make a crystallographical distinction between the *F surface*, with a ring of rhombohedron faces round the principal axis, and the *E surface* with a little star of radiating polar edges.

DISCOASTERACEAE

Discoasters are small fossils, commonly between 10 μm and 20 μm in diameter, consisting of calcite crystals grouped radially round a central axis so as to form patterns resembling rosettes or snowflakes (Pl. 89, fig. 4); these structures are commonly referred to as asteroliths. In most species the crystals lie in a single plane, which may be called the principal plane of the asterolith, at right angles to the principal axis, which behaves as an axis of symmetry for the whole body (these are the *Hauptebene* and *Hauptachse* of Stradner, in Stradner and Papp 1961, pp. 48, 49).

Optical orientation. One fundamental property of all discoasters is that their constituent crystals are invariably arranged so that the optic axis of each is parallel with the principal axis. In microscope slides prepared in the usual way, with the asteroliths lying flat against the object-glass, they remain dark between crossed nicols, and are thus easily distinguishable from coccoliths and most other nannofossils. Because of this, it has sometimes been assumed that each asterolith consists of a single crystal. This does not, however, necessarily follow from the optical behaviour, since a group of crystals with differently oriented lattices would give the same effect provided that the *c*-axes were all parallel. Examination under the electron-microscope of specimens with recognizable crystal-faces shows that as a general rule each arm of a discoaster is an independent crystal, and it is only in rather special circumstances that several rays are crystallographically united to form a single crystal.

Crystallographic observations under the electron-microscope. When discoasters are prepared by standard methods for examination under the microscope, their discoidal shape usually causes them to lie flat upon the supporting film or slide, with the principal plane at right angles to the line of vision. From their optical behaviour in polarized light we know that the trigonal axis of each crystal is then aligned parallel with the line of vision. Hence we can treat electron-micrographs of discoasters as orthographic projections on the principal plane, which coincides with the basal pinacoid {111} of the constituent crystals. This provides a convenient method of working out the development of faces on these crystals, and their relation to the general morphology of the complete discoaster. There is an additional advantage in that the plane of projection {111} is the same as that used in a conventional stereographic projection, and observations made on electron-micrographs can be quite simply related to the positions of poles and the traces of zones plotted on a standard stereogram.

On an orthographic projection, and hence on a suitably oriented electron-micrograph, all edges between faces in the same zone are represented by parallel lines, and the common direction of these lines is normal to the diameter of the zone-circle in the stereogram. By measuring the direction of a crystal-edge on an electron-micrograph we can thus find the projected direction of the zone-axis to which the adjacent faces are related. In the more simply constructed discoasters this is often all that is needed to

confirm the identity of a face recognized by inspection, for experience shows that the faces most commonly developed all have simple indices.

Occasionally the identity of a face can be settled by looking at the symmetry of etch-figures or overgrowths. For example, the basal pinacoid can often be recognized by the presence of overgrowths in the form of regular trigonal pyramids. The orientation of these pyramids fixes the cleavage directions and hence the orientation of the crystal-lattice; it also serves to distinguish (111) from ($\bar{1}\bar{1}\bar{1}$), and thus provides a means of identifying the upper and lower surfaces of an asterolith.

Simple six-armed discoasters. These principles can now be applied to some of the very simply constructed discoasters that are found in Tertiary pelagic sediments. Two species of this kind, *Discoaster adamanteus* Bramlette and Wilcoxon, and *D. obtusus* Gartner, can be obtained in an excellent state of preservation from Oligocene and Miocene deep-sea oozes. The shape of the asteroliths is determined entirely by well-developed crystal faces, the actual combination of faces varying slightly in different samples. Specimens of *D. obtusus* resembling the holotype consist of six primitive rhombohedra, and have the simplest structure possible in a six-armed discoaster (text-fig. 1; Pl. 87, figs. 3, 4). In the holotype of *D. adamanteus* the rhombohedra are modified by the addition of faces which give the asterolith a star-shaped instead of a hexagonal outline (text-fig. 2; Pl. 88, figs. 2–4). As seen under a light-microscope, the two holotypes are quite distinct in outward shape, but they are accompanied by a range of intermediate forms in which the extra faces are developed to various degrees. This leads to difficulty in drawing a line between the two species, and raises an interesting taxonomic problem.

The simplest form of *D. obtusus* is hexagonal in outline, and consists of six simple rhombohedral crystals each of which has a polar edge running radially along the middle of the arm, flanked by a pair of steeply sloping rhombohedron faces (text-fig. 1*a*; Pl. 87, fig. 4). The third rhombohedron face is directed towards the centre, and is much smaller than the other two. Measurements on suitably tilted specimens confirm the identification of the three faces on this surface of the arm as belonging to the primitive rhombohedron $\mathbf{r} = \{100\}$.

As this unequal development of individual faces belonging to the same form is found repeatedly in the arms of discoasters, it is desirable to adopt a consistent scheme for labelling such faces. For asteroliths constructed on the same plan as *D. obtusus*, with

---

EXPLANATION OF PLATE 87

Figs. 1–2. *Discoaster adamanteus* Bramlette and Wilcoxon, Middle Miocene, Trinidad (H851). 1, oblique view of *F surface*. Face (010) very small, at the centre; (100) and (001) make the flanks of the arms; (101) is not developed on the *F surface* of this specimen. 24455, ×7500. 2. Hemi-discoaster condition, orthographic view of the *F surface*. A simple combination of **r** faces without **e**. Arms 1, 3, and 5 are united to form a single crystal, with suppression of (010). In the alternate arms (010) is represented by very small triangular faces.

Figs. 3–4. *Discoaster obtusus* Gartner. 3, Hemidiscoaster condition, oblique view of *F surface*. Alternate arms are united to form a single crystal with its trigonal axis at the centre of the asterolith. (100) and (001) are the only faces developed on this surface of the arms. Lower Miocene, Jamaica (H719). 24407, ×12 500. 4, normal (Eudiscoaster) condition, orthographic view of *F surface*. Face (010) is developed as a ring of very small faces surrounding the centre. Compare text-fig. 1*a*. Lower Miocene, Pacific Ocean (H852). 24420, ×7500.

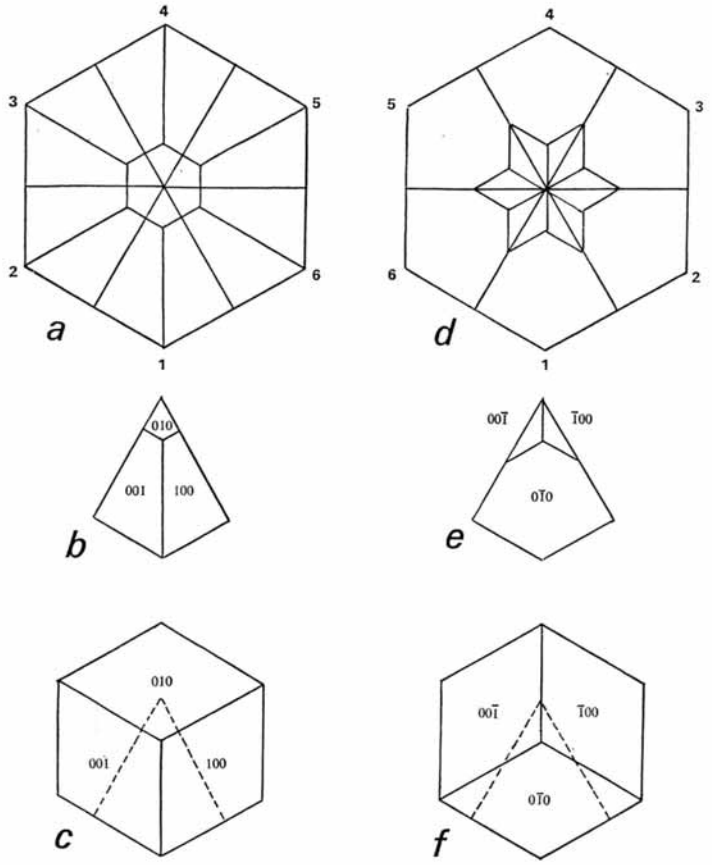

TEXT-FIG. 1. *Discoaster obtusus* Gartner in orthographic projection on (111). The asterolith consists of six arms, each of which is part of a primitive rhombohedron. *a–c. F surface* (face (010) to centre). *d–f. E surface* (edge to centre). *a, d.* The complete asterolith; compare Pl. 87, fig. 4 and Pl. 88, fig. 1. *b, e.* A single arm. *c, f.* A single arm in relation to the fully developed rhombohedron.

a crystallographic plane of symmetry running along the length of the arm (text-figs. 1, 2), the **r** face directed towards the centre is selected as (010), and the parallel face which cuts off the tip of the arm on the reverse surface of the asterolith is then (0$\bar{1}$0). The two opposite surfaces of the asterolith can thus be distinguished from each other: one has a ring of crystal faces surrounding the centre, and the other has a set of edges radiating away from it (Pl. 88, figs. 1, 2). They may conveniently be referred to as the *F surface* (face-to-centre, with positive indices for **r**) and the *E surface* (edge-to-centre, with negative indices for **r**). Specimens of *D. obtusus* almost invariably place themselves on

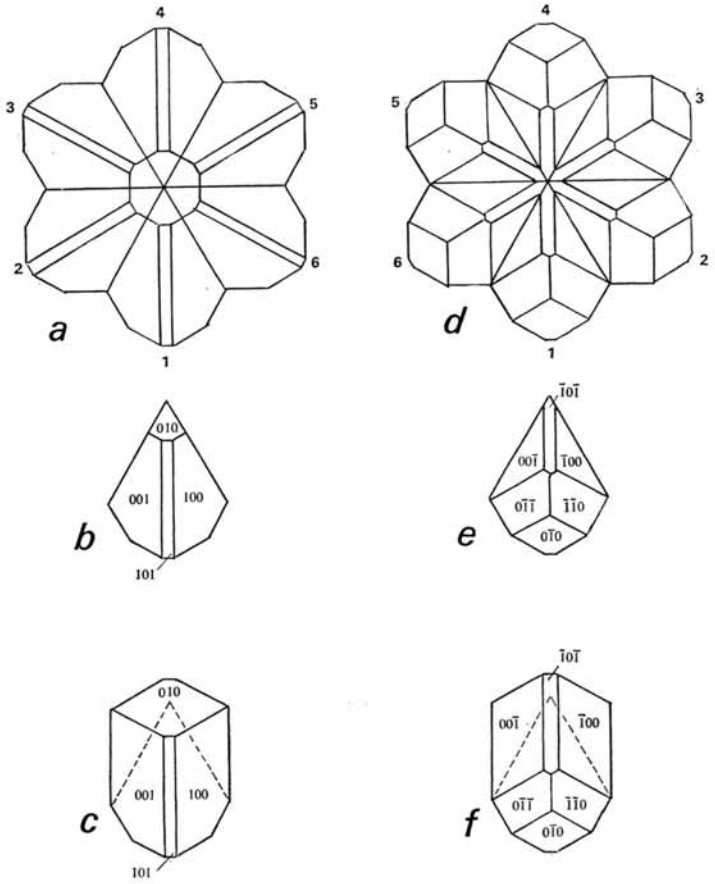

TEXT-FIG. 2. *Discoaster adamanteus* Bramlette and Wilcoxon in orthographic projection on (111). The arms are parts of crystals with a special habit combining the primitive rhombohedron **r** = {100} and the obtuse rhombohedron **e** = {101} with unequal development of the faces of both forms.

a–c. F surface. a. The complete asterolith; compare with Pl. 88, fig. 2. *b.* A single arm. *c.* A single arm in relation to the upper surface of the crystal, in which (101) is developed without (110) and (011).

d–f. E surface. d. The complete asterolith; compare with Pl. 88, fig. 4, which shows a slightly different development of faces. *e.* A single arm. *f.* A single arm in relation to the lower surface of the crystal, which unlike the upper surface includes ($\bar{1}\bar{1}$0) and (0$\bar{1}\bar{1}$).

a microscope slide with *F* uppermost because this side is steeply conical, and the fossils naturally come to rest on the flatter *E surface*.

Each of the six arms shows a similar development of faces successively rotated through an angle of 60°, and since the lattice must also be rotated through the same angle there can be no crystalline continuity between adjacent arms. In the orthographic projection

the solid angles that form the distant ends of the rays give an internal angle of 120°, and six-fold repetition produces a regular hexagon. Electron-micrographs of specimens lying flat on the supporting film show a very close approximation to this ideal shape (Pl. 87, fig. 4).

In examples of *D. adamanteus* agreeing closely with the type (Bramlette and Wilcoxon 1967, pl. 7, fig. 6) the shape of the arms is modified by additional faces belonging to the obtuse rhombohedron **e** = {110}. The six faces of this form are hardly ever all developed, and the omission of individual faces is always effected in such a way as to emphasize the bilateral symmetry of each arm (Pl. 88, fig. 3; Pl. 89, fig. 2). The crystallographic plane of symmetry running along the length of the arm thus remains operative, whereas the other two planes of symmetry are, in effect, suppressed in the external morphology of the crystal. For example, a pair of **e** faces, $(\bar{1}\bar{1}0)$ and $(0\bar{1}\bar{1})$, is conspicuously developed on the *E surface*, whereas the third face $(\bar{1}0\bar{1})$ is almost invariably suppressed (Pl. 88, fig. 4). These two faces intersect the (100) and (001) faces of the *F surface*, producing a notch in the outline of the asterolith at the distant end of each interradial suture.

In many specimens the obtuse rhombohedron is represented by the $(\bar{1}\bar{1}0)$ and $(0\bar{1}\bar{1})$ faces only, and there are no faces belonging to this form on the opposite *F surface*. Occasionally a specimen presenting the *F surface* is seen with each of the polar edges of the primitive rhombohedron **r** truncated by a narrow, parallel-sided **e** face (Pl. 88, fig. 2); more commonly, however, only (101) is developed and (110) and (011) are suppressed.

A further modification is sometimes introduced by the addition of a basal plane, either (111) or $(\bar{1}\bar{1}\bar{1})$ (Pl. 88, fig. 1). The identity of these faces can often be confirmed by the presence of little outgrowths in the shape of equilateral pyramids, which on (111) have a face and on $(\bar{1}\bar{1}\bar{1})$ an edge directed towards the centre of the asterolith.

Some of the patterns resulting from these various combinations are shown in Plates 87–89. Judged as discoasters, they all have a primitive appearance. Nevertheless, the organism has clearly exerted a firm control over the growth of its crystals, and in particular has taken considerable liberties with the trigonal symmetry of calcite to achieve some of these results. Each of the six crystals has been prevented from growing larger than a certain pre-determined size, and the pair of faces (100) and (001) has been forced to develop quite differently from (010). Although the interfacial angles necessarily preserve a trigonal symmetry, the selective development of faces gives an external form suggestive of a much lower degree of symmetry. The triad axis, all three diad axes, and two of the planes of symmetry are suppressed, leaving the third plane as the only operative element of symmetry in the crystal. This imparts a pseudomonoclinic appearance to the outward shape of each arm, mimicking a crystal of the monoclinic clinohedral class. The discoaster gives the impression of obeying the letter of crystallographic law and disregarding its spirit. This becomes more noticeable with increasing complexity of structure; indeed the elaborate shapes achieved by the more advanced discoasters are a measure of their success in overcoming the morphological limitations which trigonal symmetry imposes upon inorganically grown crystals (Pl. 89, fig. 4; Pl. 93, fig. 1).

Hemidiscoaster structure. We have already seen that there can be no crystalline continuity between adjacent arms of a six-rayed discoaster, since the crystal lattice is rotated through 60°, giving a different orientation in space. Rotation through 120°, on the other hand, brings the lattices into a parallel position, so that crystalline continuity between

alternate rays is theoretically possible. Fusion of crystals in this way does in fact take place, producing asteroliths in which three of the six rays are united to form a single crystal, separated from the alternate rays by well-marked interradial sutures (Pl. 87, figs. 2, 3; Pl. 89, fig. 2). This structure can easily be seen under a good optical microscope, and was used by Tan Sin Hok (1927, p. 120) to separate the genus *Hemidiscoaster*, with fusion of alternate rays, from *Eudiscoaster* in which all the rays retain their independence. Bramlette and Riedel (1954, p. 394) found it impossible to maintain the distinction between these two genera because several otherwise homogeneous species were found to include both variants. In fact, the special relationship between the crystals in a six-rayed asterolith would lead us to expect such a state of affairs; the possibility of crystalline continuity is always present, but it may well be a matter of chance whether it is actually achieved or not.

Pauciramous asteroliths. Some six-armed species of *Discoaster* are accompanied by a few similarly constructed asteroliths which differ in having a smaller number of arms. Some of these have been given separate specific names, but there are good reasons for regarding them as aberrant representatives of the six-armed forms which they otherwise resemble.

Just before its extinction at the end of the Pliocene Period, *D. brouweri* produced an abundance of such pauciramous forms (Pls. 90–92). These clearly are not all of the same kind. In one type, asteroliths with 3, 4, or 5 arms preserve a vestige of hexagonal symmetry in that the angles between the arms are always either 60° or 120°, and under the electron-microscope the stump of an undeveloped arm can often be seen bisecting the wider angle. Pauciramous asteroliths of this kind result simply from the failure of some

---

EXPLANATION OF PLATE 88

Fig. 1. *Discoaster obtusus*, orthographic view of *E surface*. ($\bar{1}00$) and ($00\bar{1}$) make an arrowhead pair of faces pointing towards the centre; ($0\bar{1}0$) is large, sloping outwards. The small equilateral triangles on some of the arms are ($\bar{1}\bar{1}1$). In the upper part of the figure, the median edge of the *F surface* is faintly visible through the transparent replica. Compare text-fig. 1*d*. Lower Miocene, Jamaica (H719). 24413, ×9000.

Figs. 2–4. *D. adamanteus*. Lower Miocene, Pacific Ocean (H852). 2, orthographic view of *F surface*. The ring of (010) faces makes a small hexagonal crater at the centre; (101) is narrow and not developed on all the arms. Compare text-fig. 2*a*. 22291, ×9000. 3, orthographic view of *F surface* with (101) in addition to (010), (100), and (001). 22274, ×4500. 4, orthographic view of *E surface*. ($\bar{1}00$) and ($00\bar{1}$) are developed as a pair of very small faces pointing to the centre; ($\bar{1}\bar{1}0$) and ($0\bar{1}\bar{1}$) large, ($\bar{1}0\bar{1}$) not developed; ($0\bar{1}0$) is at the outer ends of the arms, not always clearly distinguishable. Compare with text-fig. 2*d*, which differs in having the additional face ($\bar{1}0\bar{1}$). 24442, ×4500.

EXPLANATION OF PLATE 89

Fig. 1. *Discoaster* cf. *adamanteus*. *E surface*. Near the centre are ($\bar{1}00$) and ($00\bar{1}$) with the intervening edge truncated by ($\bar{1}0\bar{1}$). The lozenge-shaped face is ($\bar{1}\bar{1}\bar{1}$). ($\bar{1}\bar{1}0$) and ($0\bar{1}\bar{1}$) are relatively large. ($0\bar{1}0$) cuts off the tip of the arm. Lower Oligocene, Pacific Ocean (H861). 24051, ×4500.

Figs. 2–3. *D. adamanteus*. Lower Miocene, Pacific Ocean (H852). Hemidiscoaster condition, *F surface*. Arms 2, 4, and 6 fused to form a single crystal, arms 1, 3, and 5 independent. Each arm is a combination of (100), (001), and (101). The asterolith has three radial planes of symmetry. 24435, ×6750. 3, *D. adamanteus*, abnormal condition, *F surface*. Arm 2 is fused crystallographically with arm 6, and arm 3 with 5; 1 and 4 are still independent. Each arm is a combination of (010), (100), (001), and (101). The asterolith has only two planes of symmetry. 24444, ×4500.

Fig. 4. *Discoaster challengeri* Bramlette and Riedel, with bilaterally symmetrical arms giving radial symmetry to the asterolith. Middle Pliocene, Indian Ocean (H845). 24326, ×4500.

of the arms to grow to a normal length, and no fresh crystallographic problems are involved (Pl. 90, fig. 3–Pl. 91, fig. 3).

In a second type, there is no vestige of a hexagonal plan, and the asteroliths have a new 3-, 4-, or 5-fold symmetry with angles of 120°, 90°, or 72° between the arms (Pl. 91, fig. 4–Pl. 92, fig. 3). In asteroliths with four or five arms the general plan of construction is similar to that of six-armed individuals. Each arm is an independent crystal, separated from its neighbours by interradial sutures and presenting a similar face or edge towards the centre. The lattice having been rotated through 90° or 72° in adjacent arms, the crystals are brought into incongruent positions and have sharply defined contacts.

With three-armed asteroliths, the situation is different. By virtue of the trigonal symmetry of calcite, a rotation of 120° brings the lattices of all three arms into the same orientation. The arms then no longer behave as twinned individuals but act as a single crystal with a homogeneous lattice throughout (Pl. 92, figs. 2, 3). For this reason interradial sutures are never found in three-armed discoasters or in *Marthasterites*, which has exactly the same crystallographic structure, and differs only in the sculpturing at the tips of its arms.

Departures from radial symmetry. In the great majority of discoasters, the angle between adjacent arms is constant for any particular number of arms, so that the symmetry is truly radial around the principal axis. Occasionally individuals of *D. brouweri* are found to depart from this rule, having the six arms at unequal angles such as 30°, 60°, and 90°. Such aberrant forms have been observed in other six-armed species, and Gartner (1969, p. 598) has recently described a five-armed derivative of *D. brouweri* as a new species, *D. asymmetricus*, in which unequal spacing is the rule rather than an exception (Pl. 91, fig. 4).

When such forms are examined in detail, it is often observed that the interradial sutures are regularly disposed at angles of 60° or 72°, and that the irregular spacing is caused by a departure from bilateral symmetry in the arms themselves.

Specimens of *D. asymmetricus* from Pliocene oozes in the Pacific Ocean have interradial sutures close to 60°, 72°, and 84°, which are the sums of possible combinations of 30° and 42°, namely 30+30, 30+42, and 42+42. The arms themselves are asymmetrical, the length of the arm making angles of 30° and 42° with the interradial sutures. If all the five arms were either right-handed or left-handed, a regular spacing of 72° would result, but if arms of both kinds are combined in a single asterolith the observed angles are inevitably produced.

The six-armed specimen shown in Pl. 92, fig. 4 similarly has interradial sutures making angles of 15° and 45° with the length of the arm, and the introduction of two adjacent left-handed arms gives one angle of $15+15 = 30°$ and another of $45+45 = 90°$ instead of the normal 60°.

In asteroliths with this kind of arm, the ideal symmetry about the principal axis is of a rotary nature, and obviously cannot be strictly radial even when the arms are all spaced at equal angles. Further development of this type of construction probably leads to such forms as *D. lodoensis* with falcate arms and a much more pronounced rotary symmetry (Pl. 93, fig. 1). In these more advanced asteroliths recognizable crystal faces are almost invariably replaced by curved surfaces, and the material at present available is not suitable for crystallographic study.

BRAARUDOSPHAERACEAE

This family also builds skeletal plates consisting of crystals grouped radially round a principal axis, but it differs from the Discoasteraceae in the orientation of the crystals. In the genera under consideration, each skeletal plate consists of five units which behave optically as single crystals; for this reason the plates are usually referred to as pentaliths.

The pentalith-bearing species are customarily grouped into three genera, *Braarudosphaera*, *Micrantholithus*, and *Pemma*, but the distinctions between them are not at all sharp. It is not always easy to draw a definite line between *Pemma* and *Micrantholithus*, and some species that have been assigned to *Braarudosphaera* might equally well have been placed in one of the other genera.

In all the species so far examined, each crystal lies with one cleavage in the principal plane of the pentalith, and hence at right angles to the principal axis (Pl. 93, figs. 3, 4). For consistency of description, this cleavage is selected as (010). When the crystals are in the form of simply rhombohedra, as in *B. africana* and *M. concinnus* (Pl. 94, fig. 1; Pl. 96), they are arranged with their acute angles meeting centrally at the principal axis, and their (100) and (001) cleavages intersect at an angle of 78° on the (010) face. Hence the cleavages are not exactly parallel with the interradial sutures, which are spaced at 72°, and some adjustment is necessary to the shape of the crystals in order to make them fit compactly into a whorl of five sectors. In these two species the adjustment is made symmetrically, and this is probably true also of most species of *Micrantholithus* and *Pemma* (Pl. 94, figs. 3, 4; Pl. 95, figs. 1, 4). It is not true, however, for all species of *Braarudosphaera*, and in *B. bigelowi* there is a considerable latitude in the way that the sectors are pared down to prevent the sum of their radial angles exceeding 360°.

Optical orientation. Optically, the slow directions are arranged radially round the principal axis and the optic axes lie, not in the principal plane, but inclined to it at an angle of about 45°. From this it follows that there can be no planes of symmetry in the architecture of a pentalith, whatever the external form may suggest, the only symmetry possible being of a rotary kind around the principal axis. Pentaliths are more akin to the coccoliths in this respect than to the discoasters.

EXPLANATION OF PLATE 90

Figs. 1–4. *Discoaster brouweri* Tan Sin Hok. 1, oblique view of convex surface. Middle Pliocene, Indian Ocean (H845). 24320, ×7500. 2, orthographic view of convex surface. Lower Pliocene, Pacific Ocean (H850). 22203, ×10 000. 3, convex surface, showing unequal development of arms. Lower Pliocene, Pacific Ocean (H850). 22204, ×5000. 4, convex surface. Five-armed modification of six-armed form by failure of the sixth arm to develop fully. Upper Pliocene, Pacific Ocean (H849). 24353, ×5000.

EXPLANATION OF PLATE 91

Figs. 1–3. *D. brouweri*. 1, concave surface. Five-armed modification of six-armed form by failure of the sixth arm to develop. Middle Pliocene, Indian Ocean (H845). 24278, ×9000. 2, convex surface. Four-armed modification of six-armed form by failure of two opposite arms. Hemidiscoaster condition with fusion of alternate arms across the centre. Middle Pliocene, Indian Ocean (H845). 24299, ×6000. 3, convex surface. Three-armed modification of six-armed form, by failure of alternate arms. Upper Pliocene, Pacific Ocean (H849). 24371, ×6000.

Fig. 4. *Discoaster asymmetricus* Gartner, convex surface. This is a five-armed species with unequal spacing of the arms. Pliocene, Pacific Ocean (H728). 16984, ×9000.

In *Pemma* and *Micrantholithus* the slow direction nearly, but often not exactly, bisects the radial angle of each sector, which consequently shows approximately symmetrical extinction under the polarizing microscope. In *Braarudosphaera bigelowi* and probably in most species of this genus the extinction directions are less regular; they are not always spaced at equal angles round the principal axis, nor do they show any constant relationship to the radial edges of the sectors. Their only constant feature is that the slow-vibration direction always lies within the radial angle of each sector. Quite clearly the pentagonal symmetry suggested by the external shape of *Braarudosphaera* does not apply to the internal structure of the pentaliths. In the other two genera, the optical properties suggest a closer approximation to five-fold rotary symmetry; this is confirmed by the cleavage directions, which are often visible under the electron-microscope (Pl. 95, figs. 1–3).

Details of fine structure. The pentaliths of *B. bigelowi* have a peculiar layered structure, giving an appearance rather like the cleavage in a sheet of mica (Pl. 93, fig. 4). Each of the five segments is constructed of about 20 very thin laminae parallel with (010). Although the layering is thus parallel with one of the cleavage directions of the crystal, it is not in itself a cleavage in the mineralogical sense, since each layer is a sheet of finite thickness with sharply defined upper and lower boundaries.

The true mineral cleavage is impossible to see in well-preserved specimens. When corrosion has cut obliquely across the laminae, each layer is seen to be crossed by two sets of cleavage planes which do not pass from one lamina to the next. Apparently the calcite layers are separated from each other by some substance which prevents cleavage-fractures from passing beyond it, on the principle of laminated safety-glass. In a pentalith 2·0 μm thick the calcite laminae are about 0·1 μm in thickness, and the separating layers appear to be much thinner.

Perhaps the most remarkable feature of this arrangement is that the organism has picked out one of the three crystallographically identical cleavage directions and has treated it differently from the other two, which never show any sign of developing a comparable interlamination.

The structure within the pentalith is thus more complex than would be expected from observations in polarized light. A similar laminar structure has been observed in other species of *Braarudosphaera* and also in *Micrantholithus* and *Pemma*.

In *B. discula* (Pl. 93, fig. 2) the layered structure is much like that of *B. bigelowi*, and there is a similar inconstancy of extinction directions. In this and in most other species of the genus, the distal margins of the segments show little or no relation to crystallographic directions. The earliest known species, *B. africana* (Pl. 94, fig. 1), is exceptional in having star-shaped pentaliths whose segments have an almost unmodified rhombohedral form. Its outward shape is thus much like that of *Micrantholithus concinnus*, but without the localized thickening that is characteristic of this and other species of *Micrantholithus*.

The pentaliths of *Pemma* differ from those of other Braarudosphaeraceae by the presence of a small pit or perforation near the centre of each segment (Pl. 95, fig. 2). In polarized light they react much like the pentaliths of *Braarudosphaera*, each segment behaving as a single crystal with the slow vibration direction arranged radially. The spacing is more regular than in *Braarudosphaera*; in *P. rotundum*, the type species, each

segment is very close to 72°, and is bisected by the slow-extinction direction, usually within the accuracy of measurement.

Measurements of intersecting cleavages on the faces of the segments, if made well away from the radial sutures, always give angles close to 78° and 102°, with the acute angle towards the centre; the third cleavage (010) must therefore lie parallel to the principal plane of the fossil. The segments are laminated parallel to (010) as in *Braarudosphaera*, and this structure gives rise to striking effects in etched specimens (Pl. 95, fig. 3). Pentaliths in the Bracklesham Beds, for example, are often deeply corroded with destruction of the original outline and enlargement of the pits to form large rhomb-shaped cavities with stepped surfaces.

So far as is known, the intimate structure of *Micrantholithus* resembles that of *Pemma* in all respects. The difference between these genera lies in the outward shape of the segments and the etched forms resulting from natural corrosion. In the type species, *M. flos*, each segment has a deep triangular notch cutting into it from the circumference, leaving the segment V-shaped (Pl. 95, fig. 4). This shape is characteristic of numerous species of *Micrantholithus* in much the same way that a pit in the centre of each segment is characteristic of most species of *Pemma*.

Response to corrosion is curiously different in the three genera under review, and it is difficult to see why this should be so. In *Braarudosphaera* corrosion is apt to start at the interradial sutures, producing narrowed segments quite unlike those of the original fossil (Pl. 94, fig. 2). In *Pemma* it usually attacks the pits, which become enlarged by etching of the component laminae to produce peculiar stepped surfaces (Pl. 95, fig. 3).

EXPLANATION OF PLATE 92

Figs. 1–4. *D. brouweri*, convex surface. 1, 2, 4. Middle Pliocene, Indian Ocean (H845). 1, four-armed form showing interradial sutures. 24294, ×6750. 2, three-armed form with the arms fused into a single crystal, and no interradial sutures. 24286, ×9000. 3, corroded specimen with etch-pits. Upper Pliocene, Pacific Ocean (H849). 24364, ×4500. 4, irregular spacing of arms discussed on page 483. 24297, ×6750.

EXPLANATION OF PLATE 93

Fig. 1. *Discoaster lodoensis* Bramlette and Riedel. Asymmetrical arms giving rotary symmetry to the asterolith. Lower Eocene, Donzacq, France (H695). 15771, ×3750.

Fig. 2. *Braarudosphaera discula* Bramlette and Riedel, distal surface of slightly corroded specimen showing lamination parallel to the principal plane, (010). Lower Eocene, Donzacq, France (H695). 15782, ×6000.

Figs. 3–4. *Braarudosphaera bigelowi* (Gran and Braarud) Deflandre. 3, distal surface, which is parallel to (010). Upper Eocene, Mississippi (H696). 15750, ×9000. 4, *B. bigelowi*, proximal surface. Three sectors of a pentalith showing lamination parallel to (010). Middle Eocene, Bracklesham Bay, Sussex (H807). 19895, ×9000.

Fig. 5. *Braarudosphaera hoschultzi* Reinhardt., distal surface. Three sections of a naturally corroded pentalith with the (010) lamination picked out by differential etching. Lower Cretaceous, North Sea (H1055). 29388, ×13 000.

EXPLANATION OF PLATE 94

Figs. 1–2. *Braarudosphaera africana* Stradner. 1, distal surface of relatively undamaged specimen. Lower Cretaceous (Aptian), Alford, Lincolnshire (H599). 25334, ×4500. 2, corroded specimen. Lower Cretaceous (Albian), Mildenhall, Suffolk (H934). 26491, ×9000.

Figs. 3–4. *Pemma papillatum* Martini. Middle Eocene, Bracklesham Bay (H807). 3, non-punctate surface. 19920, ×6750. 4, punctate surface. Corroded specimen showing unilateral etching. 19893, ×6750.

The effects in *Micrantholithus* are in some respects the most remarkable of all. Species with V-shaped notches are attacked from the notch, leaving resistant bars along the interradial sutures, often more pronounced at one arm of the V than at the other.

This selective one-sided etching is most clearly seen in *M. concinnus*, which has simple unnotched rhombohedral segments (Pl. 96). The original surface in the principal plane is by definition (010), and the laminated structure within each segment is parallel with this. The (100) and (001) cleavage traces on the (010) surface are nearly parallel with the interradial sutures. Corrosion works back from the outer margin, not symmetrically, but by cutting a series of steps controlled by the intersection of the (010) and (001) cleavages, thinning the segment at one of its outer margins and leaving a thick rib along the suture which is nearly parallel with the (001) cleavage trace. The (100) cleavage plays no part at all in this effect. We thus have the extraordinary situation that the three cleavages, crystallographically indistinguishable, respond differently and quite independently to solution during the corrosion of the pentalith.

This independent behaviour of the cleavages presumably results from small-scale structural peculiarities that were built into the mineral substance of the pentaliths during the lifetime of the organism. The unique behaviour of the (010) cleavage can be readily explained by the presence of interlaminated sheets of isotropic material, which are easily seen at magnifications of a few thousand times. If, as seems likely, the different behaviour of the (100) and (001) cleavages is similarly due to associated structural features, these must be on such an extremely fine scale that magnifications up to 50 000 are not adequate to resolve them.

DISCUSSION AND CONCLUSIONS

From this brief review it is evident that although the Discoasteraceae and Braarudosphaeraceae both construct their skeletal plates by grouping a few crystals more or less symmetrically round a central axis, they have adopted fundamentally different plans for arranging these crystals and controlling their growth. The Discoasteraceae orient all their crystals with the trigonal axes parallel to the principal axis of the asterolith; elongation is at right angles to the trigonal axis, and the development of each crystal is related to a single plane of symmetry, the other two planes being suppressed. The Braarudosphaeraceae, on the other hand, arrange their crystals so that one cleavage always lies in the principal plane of the pentalith, and the optic axes are oblique to both the principal plane and the principal axis. Moreover, the calcite of each crystal is interlaminated with sheets of some other substance parallel to the (010) cleavage. The other two cleavages play a different and quite subordinate role in the structure of the pentalith.

There is thus a clear morphological difference between the two families which ought to be given taxonomic recognition in any classification based upon purely morphological characters. Deflandre (1950, p. 1158; in Piveteau 1952, p. 109) divided the Coccolithophoridae into two groups, the Heliolithae, *à structure sphérolithique*, and the Ortholithae, *à structure crystalline*. These two groups have come to be treated as orders, the coccoliths proper being placed in the Heliolithae, and the discoasters and braarudosphaeres united together in the Ortholithae. The fossils of both groups are of course all crystalline, the *structure sphérolithique* being merely a special way of arranging the crystals in which a rotary symmetry is usually involved. We have seen that rotary symmetry is also characteristic of the Braarudosphaeraceae which, in this respect, have

more in common with the coccoliths than with the discoasters, whose symmetry is prevalently radial. The distinction between Heliolithae and Ortholithae, useful though it was at the time of its original introduction, now needs reconsideration in view of our more detailed knowledge of fine structure.

The structural and crystallographical differences between the Discoasteraceae and Braarudosphaeraceae clearly result from biological controls which the living cells were able to exert over the crystallization of calcite. Research into the nature of these controls by biochemical methods is ruled out as far as the Discoasteraceae are concerned, for this family appears to be totally extinct. There is, however, one species of the Braarudosphaeraceae still living, and an investigation of carbonate secretion in cultures of *B. bigelowi* is needed to discover the biochemical conditions within the cell that enable the organism to differentiate between crystallographic directions that are indistinguishable according to inorganic laws. The purely palaeontological evidence reviewed above cannot carry us very far along this line of inquiry, but it does nevertheless give a glimpse of the structural devices by which the properties of calcite can be modified without interfering with the crystal lattice.

Acknowledgements. It is a pleasure to thank Professor P. Allen for reading the manuscript, and for his many helpful suggestions.

Carbon replicas for the illustrations were prepared and photographed by Mr. D. Stubbings, using an A.E.I. EM6 electron-microscope provided by D.S.I.R. (now N.E.R.C.). Prints are by Mrs. Rolfe and Mr. M. H. Waring.

I am most grateful to the Council of Trinity College, Cambridge for a generous contribution towards the cost of publication of this paper.

REFERENCES

BLACK, M. 1963. The fine structure of the mineral parts of the Coccolithophoridae. *Proc. Linn. Soc. London*, **174**, 41–46.

BRAMLETTE, M. N., and MARTINI, E. 1964. The great change in calcareous nannoplankton fossils between the Maestrichtian and Danian. *Micropaleontology*, **10**, 291–322.

—— and RIEDEL, W. R. 1954. Stratigraphic value of discoasters and some other microfossils related to recent coccolithophores. *J. Paleont.* **28**, 385–403.

—— and SULLIVAN, F. R. 1961. Coccolithophorids and related nannoplankton of the early Tertiary in California. *Micropaleontology*, **7**, 129–188.

—— and WILCOXON, J. A. 1967. Middle Tertiary calcareous nannoplankton of the Cipero section, Trinidad, W.I. *Tulane Stud. Geol.* **5**, 93–131.

EXPLANATION OF PLATE 95

Figs. 1–3. *Pemma rotundum* Klumpp. Middle Eocene, Bracklesham Bay (H807). 1, non-punctate surface with rosette of rhombohedra indicating crystal-orientation. The visible face of each crystal is (0$\bar{1}$0). 19867, ×4500. 2, punctate surface, slightly corroded and showing pits of normal size. Relics of the original (010) surface are preserved near the centre. 19908, ×4500. 3, punctate surface, deeply corroded with great enlargement of the pits and displaying lamination parallel with (010). The (100) and (001) cleavage directions are picked out near the periphery. 19894, ×6750.

Fig. 4. *Micrantholithus pinguis* Bramlette and Sullivan. Upper Paleocene, Lodo Canyon, California (H1053). 28674, ×9000.

EXPLANATION OF PLATE 96

Fig. 1. *Micrantholithus concinnus* Bramlette and Sullivan, corroded specimen showing internal lamination parallel with (010) and the effects of unilateral corrosion controlled by the intersection between this lamination and the (001) cleavage. Upper Paleocene, Lodo Canyon, California (H1053). 28663, ×11 000.

DEFLANDRE, G. 1934. Les Discoastéridés, microfossiles calcaires incertae sedis. *Bull. Soc. franç. micr.* **3,** 59–67.

—— 1947. *Braarudosphaera* nov. gen., type d'une famille nouvelle de coccolithophoridés actuels à éléments composites. *C. R. Acad. sc.* Paris, **225,** 439–441.

—— 1950. Observations sur les coccolithophoridés, à propos d'un nouveau type de braarudosphaeridé, *Micrantholithus*, à éléments clastiques. Ibid. **231,** 1156–1158.

—— 1952. Classe de coccolithophoridés, *in* J. PIVETEAU, *Traité de paléontologie*, **1,** 107–115. Paris: Masson.

GARTNER, S. 1967. Calcareous nannofossils from Neogene of Trinidad, Jamaica and Gulf of Mexico. *Univ. Kan. Paleont. Contrib.*, Paper **29,** 1–7.

—— 1969. Correlation of Neogene planktonic foraminifer and calcareous nannofossil zones. *Trans. Gulf-Cst. Ass. geol. Socs.* **19,** 585–599.

MANIVIT, H. 1965. Nannofossiles calcaires de l'Albo-Aptien. *Rev. micropaléont.* **8,** 189–201.

MARTINI, E. 1965. Mid-Tertiary calcareous nannoplankton from Pacific deep-sea cores. *Colston Papers,* **17,** 393–411.

—— and BRAMLETTE, M. N. 1963. Calcareous nannoplankton from the experimental Mohole drilling. *J. Paleont.* **37,** 845–856.

NOËL, D. 1960. Revision du genre *Discoaster* Tan Sin Hok. *Bull. Soc. Hist. nat. Afr. Nord,* **51,** 201–299.

PAASCHE, E. 1968. Biology and physiology of coccolithophorids. *Annual Review of Microbiology,* **22,** 71–86.

ROTH, P. H. 1970. Oligocene calcareous nannoplankton biostratigraphy. *Ecl. Geol. Helv.* **63,** 799–881.

STRADNER, H. 1963. New contributions to Mesozoic stratigraphy by means of nannofossils. *Proc. Sixth World Petrol. Congr.*, Sec. **1,** 167–183.

—— and PAPP, A. 1961. Tertiäre Discoasteriden aus Österreich und deren stratigraphischen Bedeutung. *Jahrb. Geol. Bundesanst. Wien,* Sonderbd. **7,** 1–159.

TAN SIN HOK. 1927. Over de sammenstellung en het onstaan van krijt en mergelgesteenten van de Molukken. *Jaarb. Mijnw. Nederl.-Indie,* **55,** 1–165.

WATABE, N., and WILBUR, K. M. 1966. Effects of temperature on growth, calcification, and coccolith form in *Coccolithus huxleyi* (Coccolithineae). *Limnol. Oceanogr.* **11,** 567–575.

M. BLACK
Department of Geology
Sedgwick Museum
Downing Street
Cambridge CB2 3EQ

Typescript received 13 October 1971

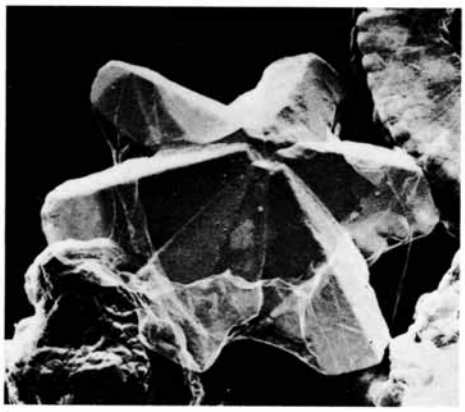

1

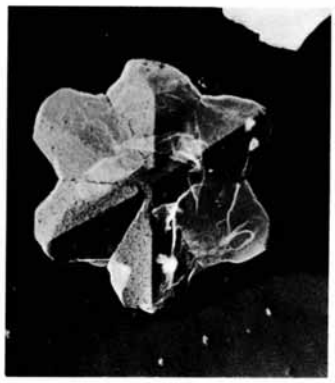

2

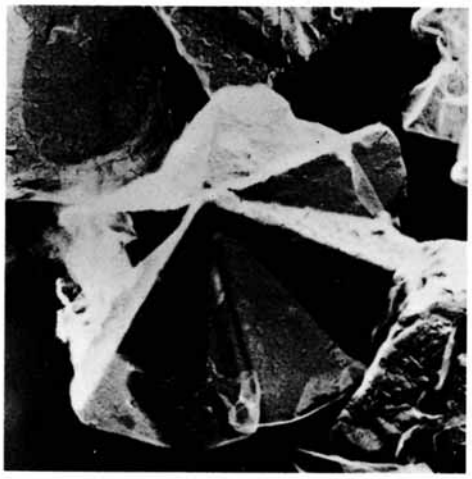

3

4

BLACK, Planktonic algae

1

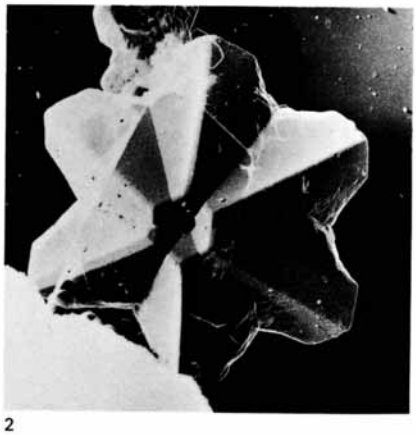

2

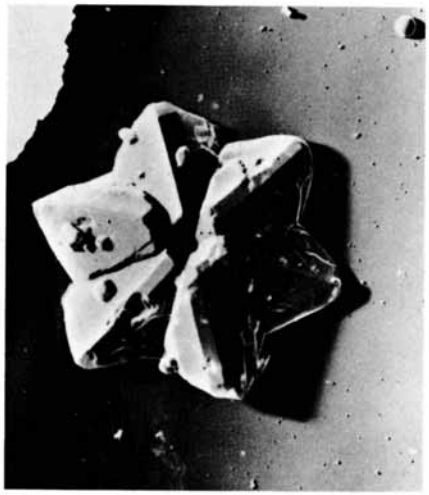

3

4

BLACK, Planktonic algae

1

2

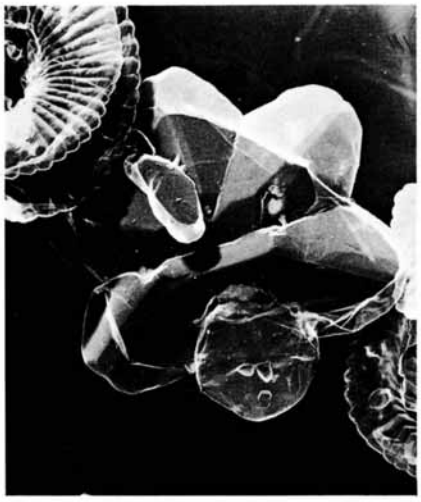

3

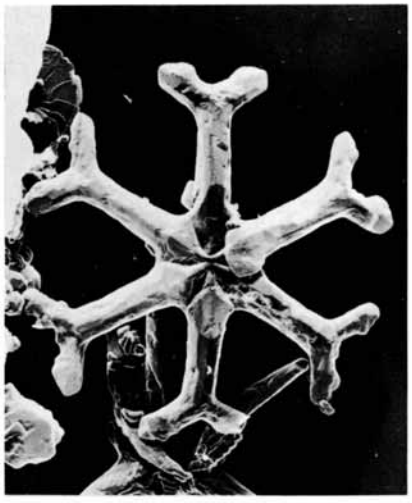

4

BLACK, Planktonic algae

1

3

2

4

BLACK, Planktonic algae

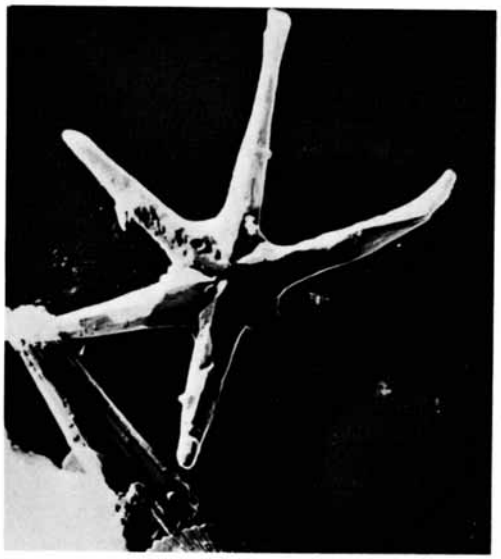

1

2

3

4

BLACK, Planktonic algae

1

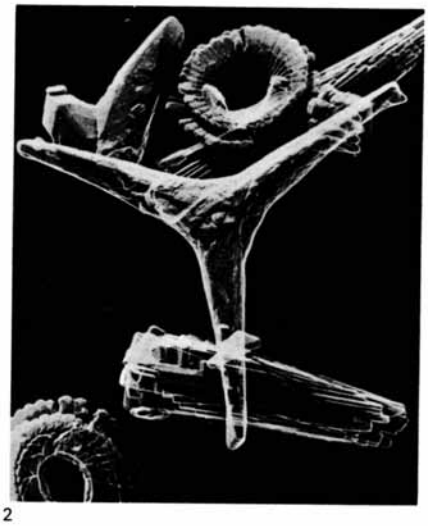

2

3

4

BLACK, Planktonic algae

1

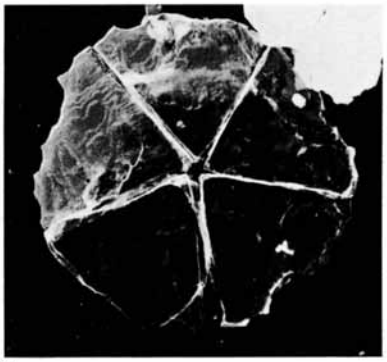

2

4

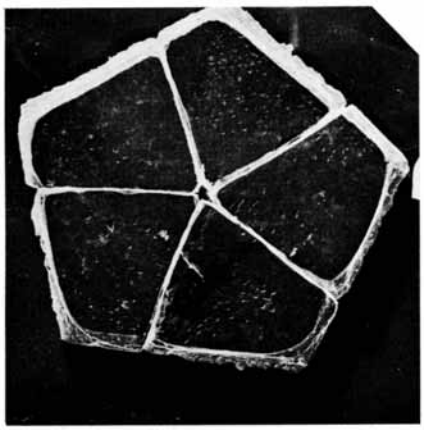

3

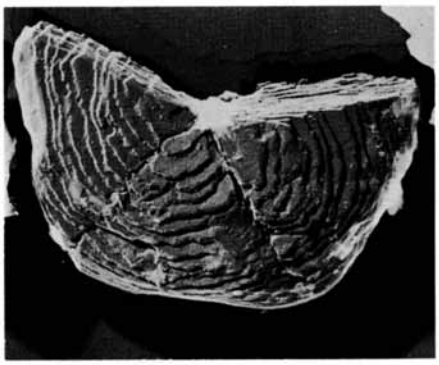

5

BLACK, Planktonic algae

1

2

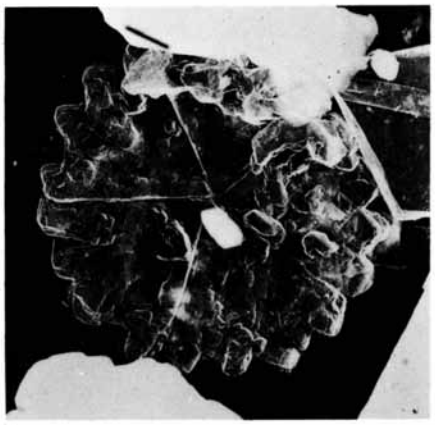

3

4

BLACK, Planktonic algae

1

2

3

4

BLACK, Planktonic algae

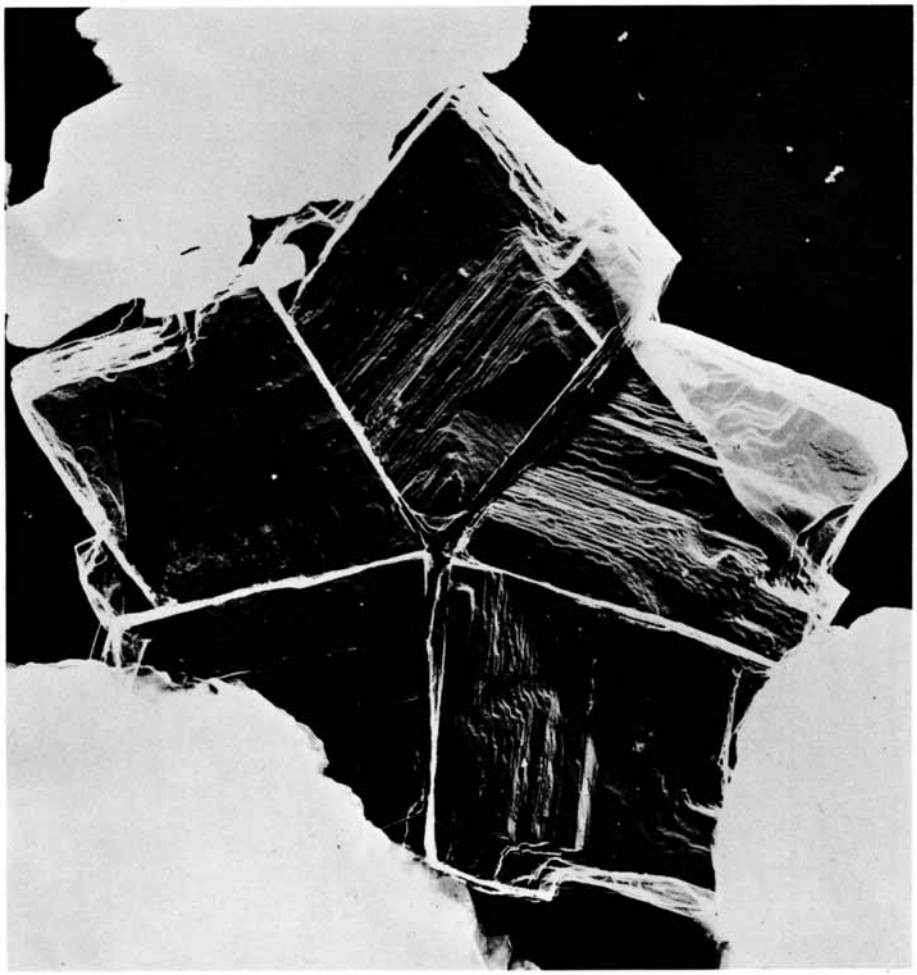

BLACK, Planktonic algae